

Supplementary Information

A periodontal tissue regeneration strategy via biphasic release of zeolitic imidazolate framework-8 and FK506 using a uniaxial electrospun Janus nanofiber

Maolei Sun,^a Yun Liu,^a Kun Jiao,^a Wenyuan Jia,^b Kongzhao Jiang,^a Zhiqiang Cheng,^c Guomin Liu,^{*b}
and Yungang Luo^{*a}

^a Department of Stomatology, the Second Hospital of Jilin University, Changchun 130041, P. R. China

^b Department of Orthopedics, the Second Hospital of Jilin University, Changchun 130041, P. R. China

^c College of Resources and Environment, Jilin Agriculture University, Changchun 130118, P. R. China

*** Correspondence authors:**

Guomin Liu, Department of Orthopedics, The Second Hospital of Jilin University, No. 218 Ziqiang Street, Changchun 130041, P. R. China. E-mail: liuyedao123@163.com

Yungang Luo, Department of Stomatology, The Second Hospital of Jilin University, No. 218 Ziqiang Street, Changchun 130041, P. R. China. E-mail: luoygjl@sina.com

Methods

Preparation of ZIF-8 nanoparticles

ZIF-8 nanoparticles (ZIF-8 NPs) was carried out at room temperature as reported, previously.¹ In brief, 1.17 g Zn (NO)₃·6H₂O, dissolved in 8 g of deionized (DI) water was added to 22.7 g 2-methylimidazole dissolved in 80 g DI water. The reaction solution was stirred at room temperature for ~ 5 min. After that, the produce was isolated via centrifugation, washed with deionized DI water and dried in a vacuum oven. The morphology of ZIF-8 NPs was obtained by transmission electron microscopy (TEM, JOEL JEM-201). The information on the crystalline phase structure of ZIF-8 NPs was obtained by X-ray diffractometer (XRD, SmartLab SE). The functional groups of ZIF-8 NPs were measured by Fourier transform infrared spectrometer (FTIR, FTIR-650).

Results

Characterization of ZIF-8 NPs

The morphology of ZIF-8 NPs was rhombic dodecahedral in shape and the size distribution was 110.58±9.39 nm (Fig. S1-S2). The XRD pattern of the synthesized ZIF-8 NPs were in good agreement with the simulated crystal image, suggesting a pure phase of the synthesized ZIF-8 NPs (Fig. S3). The FT-IR spectrum showed the peak positions and their assignments agreed well with those reported in the literature (Fig. S4).² These results showed the successful synthesis of ZIF-8 NPs and can be used without further purification.

Figures

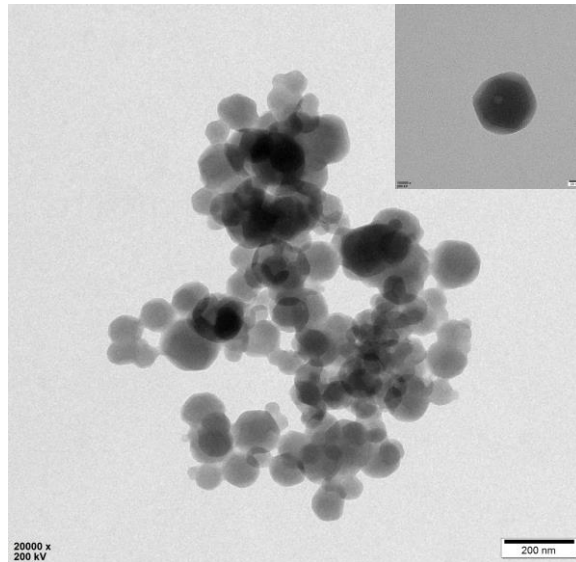


Fig. S1. TEM images of ZIF-8 NPs.

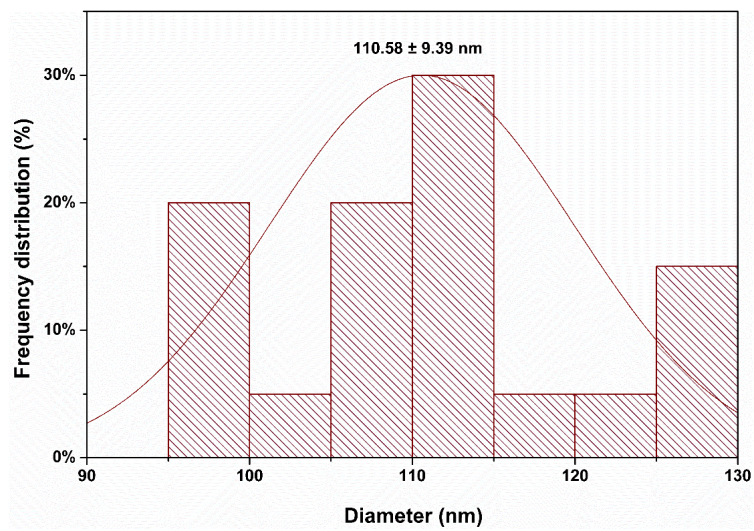


Fig. S2. Size distribution of the ZIF-8 NPs.

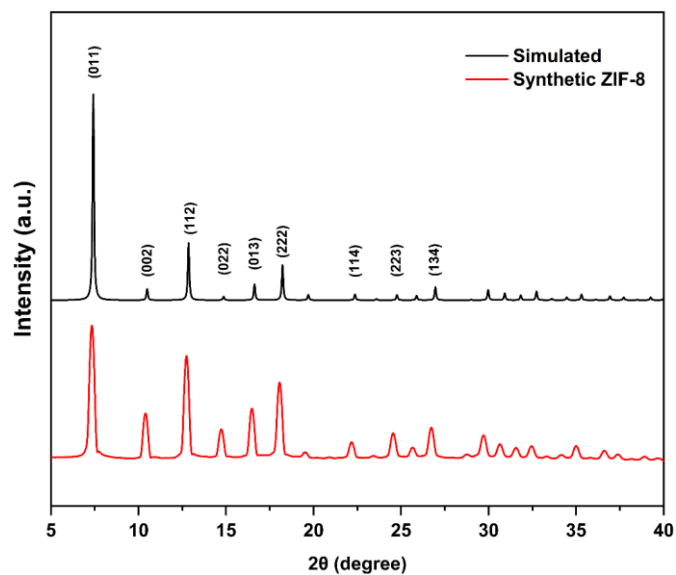


Fig. S3. XRD patterns of the ZIF-8 NPs.

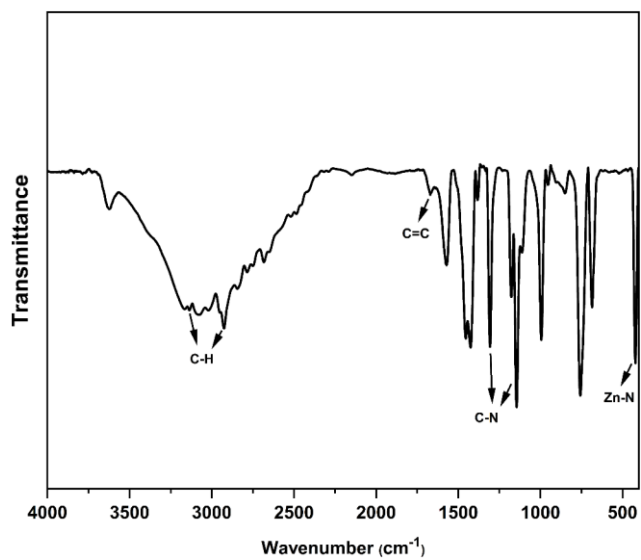


Fig. S4. FT-IR spectra of the ZIF-8 NPs.

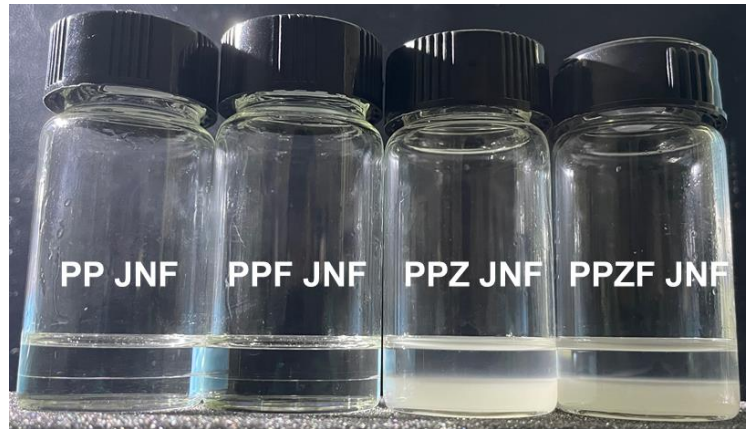


Fig. S5. The phase separation phenomenon in precursor solution.

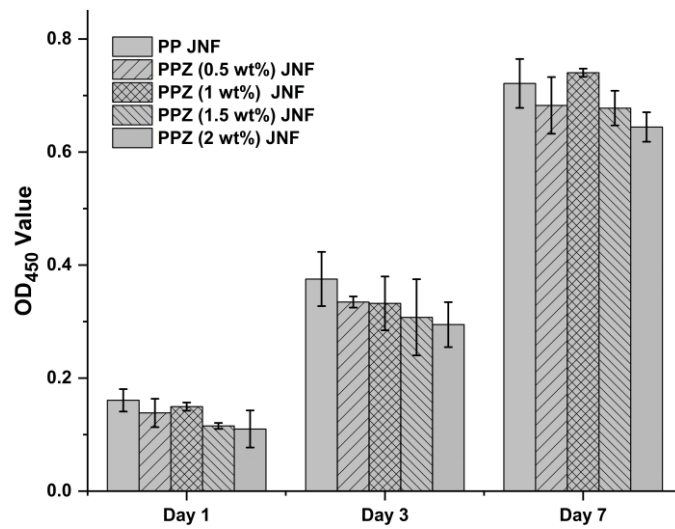


Fig. S6. Proliferation of BMSCs on PP Janus nanofibers and PPZ Janus nanofibers with different concentrations of ZIF-8 NPs. Data are presented as means \pm SD. * $P < 0.05$, ** $P < 0.01$, *** $P < 0.001$.

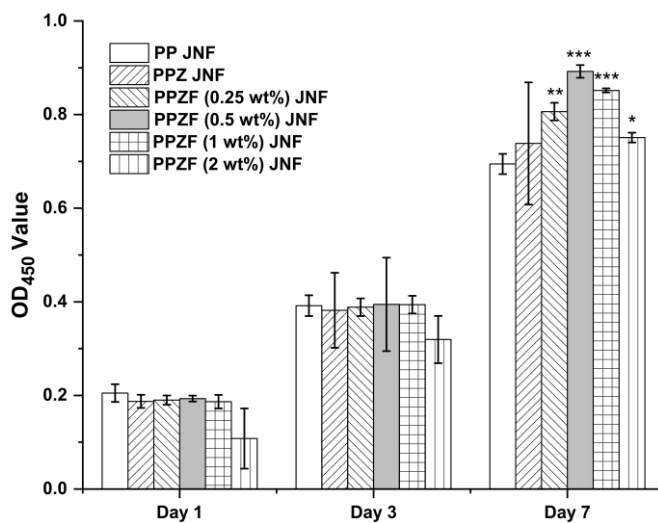


Fig. S7. Proliferation of BMSCs on PP Janus nanofibers, PPZ Janus nanofibers, and PPZF Janus nanofibers with different concentrations of FK506. Data are presented as means \pm SD. * $P < 0.05$, ** $P < 0.01$, *** $P < 0.001$.

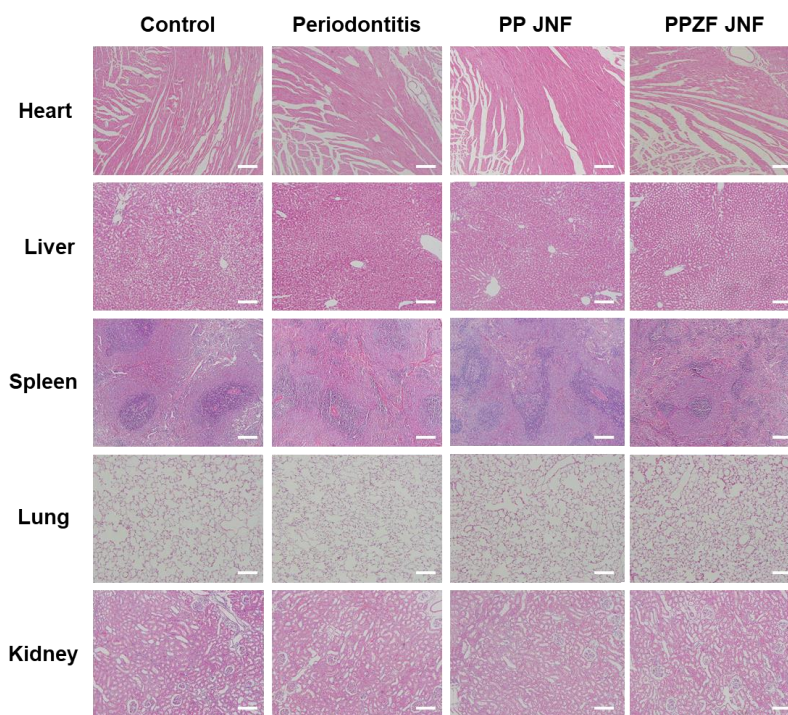


Fig. S8. H&E staining of vital organs including hearts, livers, spleens, lung and kidneys. Scale bar is 10 μm .

Table

Table S1. Primer Sequences of the Genes Involved in this Study

primer	sequence (5' to 3')
rat- <i>β-actin</i> -F	GGAGATTACTGCCCTGGCTCCTA
rat- <i>β-actin</i> -R	GACTCATCGTACTCCTGCTTGCTG
rat- <i>Runx2</i> -F	CATGGCCGGGAATGATGAG
rat- <i>Runx2</i> -R	TGTGAAGACCGTTATGGTCAAAGTG
rat- <i>Osx</i> -R	CATCCATGCAGGCATCTCA
rat- <i>Osx</i> -R	CTGCCACACCTAACCAA
rat- <i>Alp</i> -F	CATCGCCTATCAGCTAATGCACA
rat- <i>Alp</i> -R	ATGAGGTCCAGGCCATCCAG
rat- <i>Ocn</i> -F	TTATTGTTTGAGGGGCCTGGG
rat- <i>Ocn</i> -R	TGCTCCTACAAAGCTGTCTCC

References

- 1 Y. C. Pan, Y. Y. Liu, G. F. Zeng, L. Zhao, Z. P. Lai, *Chem. Commun.*, 2011, **47**, 2071-2073.
- 2 S. R. Venna, M. A. Carreon, *J. Am. Chem. Soc.*, 2010, **132**, 76-78.